

UDC 669.018.25:621.785.5:621.793.6:669.781

## A STUDY OF BORONIZING KINETICS AND ITS EFFECT ON THE STRUCTURE AND MECHANICAL PROPERTIES OF STEEL 16MnCr5

Adnan Calik,<sup>1</sup> Nazim Ucar,<sup>2</sup> and Nuri Yeniay<sup>1</sup>

Translated from *Metallovedenie i Termicheskaya Obrabotka Metallov*, No. 1, pp. 62 – 67, January, 2022.

*Original article submitted May 5, 2021.*

The kinetics of boronizing of low-alloy steel 16MnCr5 at 1123, 1173 and 1223 K for 2, 4 and 6 h in powder mixtures using the Ekabor-II agent is studied for determining the possibility of raising the surface properties of this steel. The microstructure is studied using optical and electron microscopy and x-ray diffractometry. The mechanical properties of the steel boronized by different variants are analyzed. It is shown that the growth of the boride layer with time obeys a parabolic dependence. The activation energy of boron diffusion and the pre-exponential factor are determined. An empirical equation is obtained for predicting the thickness of boronized layer on steel 16MnCr5 as a function of the temperature and time of the boronizing. Boronizing is shown to increase the yield strength and the ultimate tensile strength of the steel at lowering of the ductility. Boronizing at 1223 K for 6 h produces a boronized layer with a hardness of 1940  $HV_{0.1}$  at a hardness of the matrix equal to 401  $HV_{0.1}$ .

**Key words:** boronizing (boriding), steel 16MnCr5, kinetics, activation energy, mechanical properties.

### INTRODUCTION

Alloy steel 16MnCr5 (AISI 7131) has a favorable combination of high impact toughness of the core and enough strength of the surface and is used widely for production of automobile components such as gears, shaft and crankshafts [1 – 3]. The operating properties of this steel are mainly advanced by heat treatment (carburizing) and thermomechanical surface hardening (boronizing) [4 – 6]. A recent technique for raising the impact toughness of steel 16MnCr5 consists in elevation of the content of manganese and lowering of the concentration of carbon. However, it has been shown in [7] that reduction of the content of C, N, Si, Cr and Mo and addition of Ni, Cu and Mn lower substantially the hardness and the strength of alloy steels. An alternative method for improving the combination of mechanical properties of steel 16MnCr5 is heat treatment. In [4], the microhardness of this steel is shown to attain 720  $HV$  and the ultimate

strength  $\sigma_r = 387$  MPa after carburizing. In [1], the hardness and the wear resistance of steel 16MnCr5 carburized and then treated at cryogenic temperatures grow and the impact toughness decreases.

Boronizing (boriding) is used in industry as widely as carburizing for prolonging the service, lowering the coefficient of friction and raising the wear and corrosion resistances of steels without degradation of high mechanical properties [8 – 10]. However, despite the numerous studies of the structure and properties of low-alloy steel 16MnCr5 [1, 2, 4, 11, 12], detailed investigations of the effect of boriding on the properties of this steel are quite scarce. The influence of continuous and interrupted boriding treatments on the properties of steel 16MnCr5 has been studied in [13]. It has been shown that boriding produces a strong effect on the hardness and microstructure of the steel, and the continuous variant raises its hardness more efficiently.

The aim of the present work was to perform a detailed analysis of the kinetics of boriding and its effect on the microstructure and phase composition of the surface layer and on the mechanical properties of low-alloy steel 16MnCr5.

<sup>1</sup> Isparta University of Applied Sciences, Faculty of Technology, Mechanical Engineering, Isparta, Turkey.

<sup>2</sup> Faculty of Arts and Sciences, Physics Department, Suleyman Demirel University, Isparta, Turkey (e-mail: nazimucar@sdu.edu.tr).

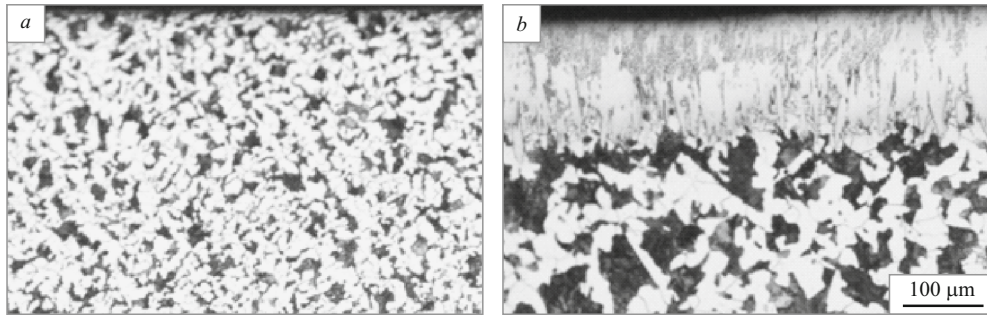


**Fig. 1.** Microstructure in cross section of a specimen of steel 16MnCr5 in initial condition (a) and after boriding at 1173 K for 6 h (b).

## METHODS OF STUDY

We studied steel 16MnCr5 of the following chemical composition (in wt.%): 0.16 C, 1.15 Mn, 0.87 Cr, 0.24 Si, 0.02 S, 0.012 P. The specimens cut from a billet were annealed for removing the internal stresses.

Boriding was conducted in a solid environment, i.e., a powder mixture, using an Ekabor-II agent at atmospheric pressure in electric resistance furnaces at 1123, 1173 and 1223 K for 2, 4 and 6 h. The microstructure of the polished and etched specimens was studied in a cross section with the help of an optical microscope and a JEOL 5600 LV scanning electron microscope. The thickness of the borided layer was determined using a digital meter attached to the optical microscope (Nikon MA100). The phase composition was determined using an x-ray diffractometer (Rigaku D-MAX 2200) in copper  $K_{\alpha}$  radiation ( $\lambda = 0.015418$  nm). The microhardness was measured using a TTS Matsuzawa HWMMT-X3 hardness tester at a load of 100 g on the indenter with a hold for 10 sec. The static tensile tests were conducted using an Instron Himadzu AGS-X machine with maximum permissible load 10 kN in accordance with the ASTM-E8M standard for specimens with design length 15 mm. We determined the conventional yield strength  $\sigma_{0.2}$ , the ultimate strength  $\sigma_r$  and the ductility parameters. The Charpy impact bending tests were conducted using an Instron Ceast 9350 pendulum impact machine with maximum impact energy 300 J in accordance with ASTM-E23.

## RESULTS AND DISCUSSION

Figure 1 presents the structure of steel 16MnCr5 in the initial condition and after boriding at 1173 K for 6 h. In the initial condition the structure is represented by ferrite (the light matrix) and pearlite (the dark inclusions). Boriding produces a dense homogeneous boride layer on surface of the steel, and the structural components (ferrite and pearlite) become coarser.

Figures 2 and 3 present cross sections of specimens borided by different variants. The images of the structure under high magnification (Fig. 3) prove formation of a compact and homogenous coating on the surface of the steel. It can also be seen that the thickness of the boride layer increases with increase of the temperature and prolongation of the boriding process; the boride layer is the thicker, the higher the temperature and the longer the process. We determined the average thickness of the boride layer for each boriding mode after making 15 measurements. The highest thickness (159  $\mu\text{m}$ ) was obtained after the treatment at 1223 K for 6 h. Figure 4 presents the dependences of the thickness of the boride layer on  $\sqrt{t}$ , where  $t$  is the time of the treatment. The dependence has a parabolic nature.

Deciphering of the x-ray patterns obtained after boriding of steel 16MnCr5 shows that the main phases formed in the surface layer are FeB at the surface and  $\text{Fe}_2\text{B}$  near the matrix (Fig. 5). In addition, the patterns obtained after boriding at 1223 K for 6 h exhibit peaks corresponding to  $\text{Cr}_2\text{B}$  and

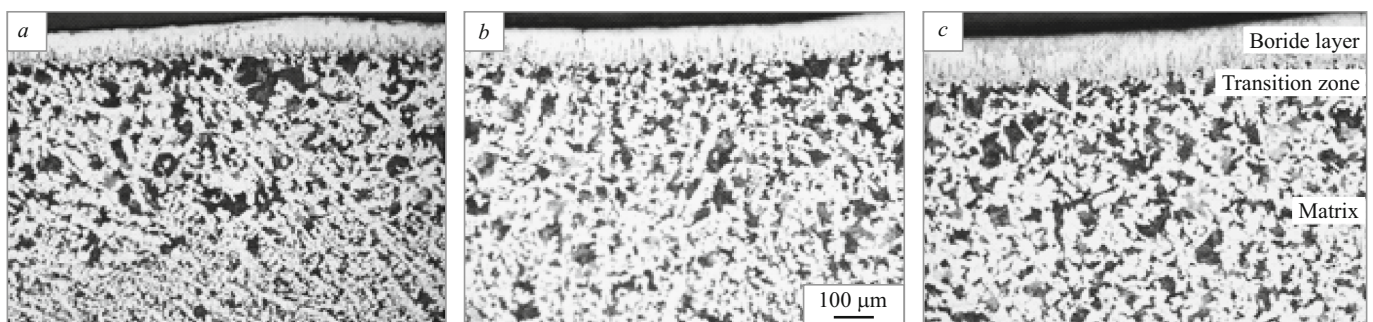


**Fig. 2.** Microstructure of steel 16MnCr5 (cross section of a specimen) after boriding at 1223 K for 1 h (a), 4 h (b) and 6 h (c).

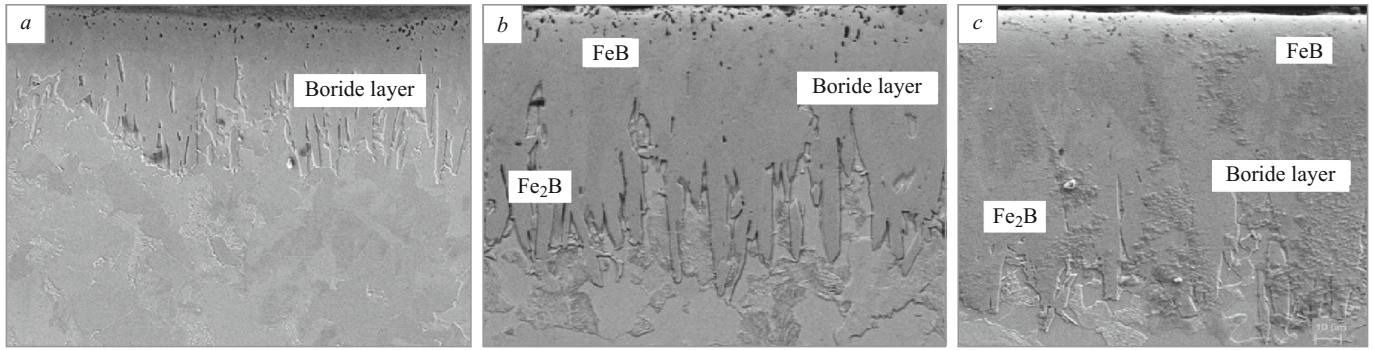


Fig. 3. Structure of boride coatings (cross section, SEM) on steel 16MnCr5 after 6-h boriding at 1123 K (a), 1173 (b) and 1223 K (c).

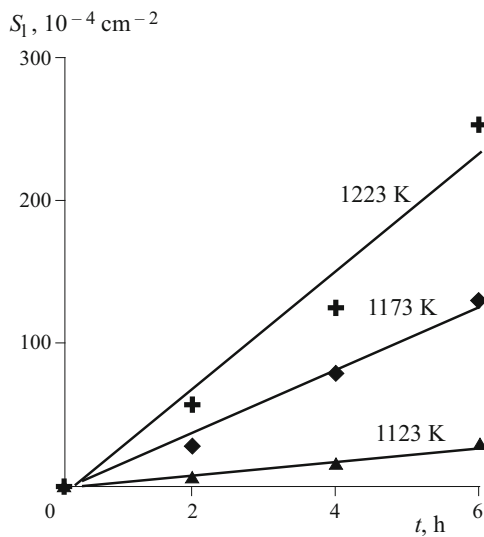


Fig. 4. Dependence  $S_1 = f(t^{1/2})$  (where  $S_1$  is the squared thickness of the boride layer and  $t$  is the boriding time) for steel 16MnCr5 borided at different temperatures (given at the curves).

MnB borides (Fig. 5b), which is explainable by the high content of Mn and Cr in the steel.

The microhardness was measured in cross sections of the specimens at different distances from the surface up to the matrix. Then we calculated the average value of the microhardness after five measurements at each depth (Fig. 6). The maximum hardness (1940  $HV_{0.1}$ ) was obtained after boriding at 1223 K for 6 h, which is about 5 times higher than in the steel in the initial condition. This considerable growth in the surface hardness of the metal is connected with formation of MnB and  $Cr_2B$  manganese and chromium borides in addition to the hard FeB and  $Fe_2B$  iron borides and with strong distortion of the crystal lattice due to formation of a solid solution of boron in iron. The same explanations can be found in [14 – 16]. It should also be noted that the hardness of the studied borided steel is very close to the values obtained for low-alloy steels under similar boriding conditions, i.e., 1759  $HV_{0.1}$  for 16MnCr5 borided at 1273 K for 16 h in [13], 1610  $HV_{0.1}$  for AISI 8620 borided at 1210 K for 4 h in

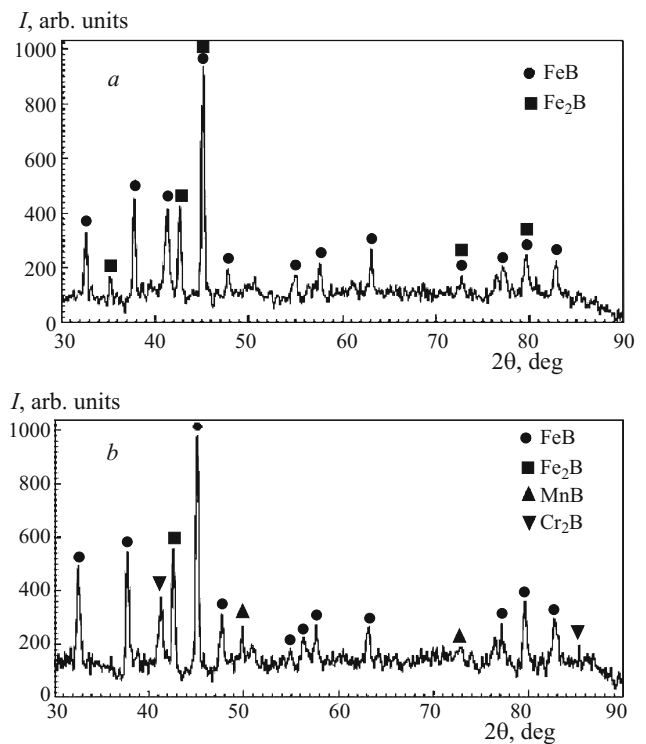
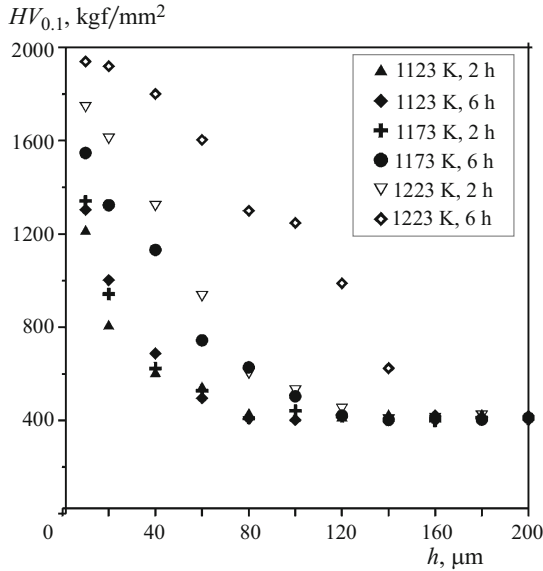


Fig. 5. Diffraction patterns of the surface layer of steel 16MnCr5 after boriding at 1123 K for 2 h (a) and at 1223 K for 6 h (b).

[17], and 2030  $HV_{0.1}$  for AISI 4130 borided at 2213 K for 5 h in [18].

Table 1 presents the results of the determination of mechanical properties of steel 16MnCr5 in the initial condition and after different variants of boriding. It can be seen that boriding elevates considerably the strength of the metal but lowers somewhat the ductility. It can be assumed that the effect of the treatment on  $\sigma_{0.2}$  and  $\sigma_1$  is explainable not only by formation of hard iron borides in the surface layer but also by the presence of  $Cr_2B$  and MnB borides. It has been shown in [19] that inclusions of a  $Fe_{1.1}Cr_{0.9}B_{0.9}$  boride in the structure of a stainless steel with a high boron content raise substantially its strength characteristics. It also follows from Table 1 that boriding raises the fracture energy under impact bending



**Fig. 6.** Measured values of microhardness over the thickness of a specimen ( $h$  is the distance from the surface) of steel 16MnCr5 after boriding at 1123, 1173 and 1223 K for 2 and 6 h.

of the steel by a factor of 2 – 4 depending on the treatment mode. These results show that an optimum combination of mechanical properties in steel 16MnCr5 can be obtained by varying the boriding parameters (the temperature and the duration).

It should be noted that published reports on the effect of boriding on the mechanical properties of materials are contradictory. In some cases, the values of  $\sigma_{0.2}$  and  $\sigma_r$  of the steel decrease after boriding due to formation of a hard but brittle surface layer [20, 21]. In other works, it is shown that  $\sigma_{0.2}$  and  $\sigma_r$  increase after boriding, and the elongation decreases [22, 23].

It is known that the choice of the parameters of the boriding process is based on the knowledge of the kinetics of growth of the surface layer. In the last twenty years the kinetics of growth of boride layers in various steels has been studied by many researchers [14, 24 – 27]. It has been shown that boride layers grow in the direction of the diffusion flow

**TABLE 1.** Mechanical Properties of Steel 16MnCr5 Borided by Different Variants

$T$ , K	$t$ , h	$\sigma_{0.2}$ , MPa	$\sigma_r$ , MPa	$\delta$ , %	$A$ , J
Without boriding	–	180	440	27	36
1123	6	300	610	14	69
1223	6	370	710	8	115
1173	2	180	530	21	51
1173	6	320	670	7	97

**Notations:**  $T$  is the boriding temperature;  $t$  is the boriding duration;  $A$  is the fracture energy in the impact tests.

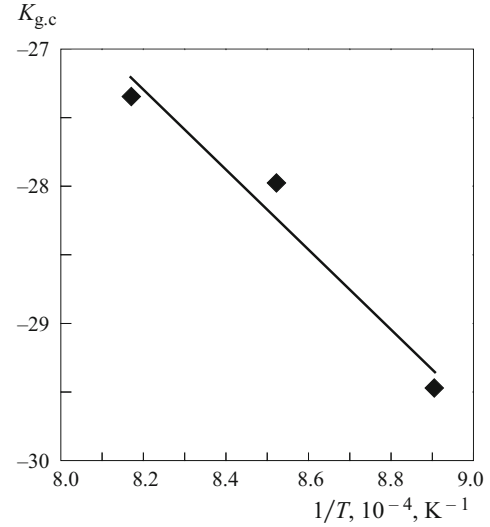


**Fig. 7.** Rate of growth of coating  $K_{g,c}$  on steel 16MnCr5 as a function of reciprocal temperature of boriding  $1/T$ .

of boron atoms perpendicularly to the surface of the substrate and the growth is describable by a parabolic dependence

$$d^2 = Kt, \quad (1)$$

where  $d$  is the thickness of the boride layer (m),  $t$  is the duration of the boriding (sec), and  $K$  is the constant of the rate of parabolic growth at the specified boriding temperature ( $m^2/sec$ ). Consequently,  $K$ ,  $Q$ , and  $T$  (K) may be related through the Arrhenius equation

$$K = K_0 \exp\left(-\frac{Q}{RT}\right), \quad (2)$$

where  $K_0$  is the collision factor (also known as a pre-exponential factor dependent on the boron potential in the saturating medium) ( $m^2/sec$ );  $Q$  is the activation energy (J/mole);  $T$  is the absolute temperature (K), and  $R$  is the universal gas constant (J/(mole · K)).

The dependence of  $\ln K$  on reciprocal temperature (Fig. 7) allows us to calculate the activation energy  $Q$  and the collision factor  $K_0$  from the slope of the curve and its intersection with the  $Y$ -axis ( $y$ -intercept), respectively. In the case of boriding of steel 16MnCr5  $Q = 243.6$  kJ/mole and  $K_0 = 3.75 \times 10^{-2}$   $m^2/sec$ . Since we have not found published data on the kinetics of boriding of steel 16MnCr5, we can compare the results obtained only with the data reported for steels of other grades. For low-alloy steels with chemical composition close to that of 16MnCr5 the activation energy has been determined to be 189.4 [28], 215 [29], 158.78 [30], 194.3 [31], and 213.9 kJ/mole [32] for borided steels AISI 4140 (pack boriding at 1123 – 1273 K), AISI 4140 (in salt bath at 1123 – 1223 K), AISI 4140 (in a powder mixture at 1123 – 1273 K), AISI P20 (pack boriding at 1123 – 1223 K) and AISI P20 (with the use of microwave radiation at

1123 – 1223 K), respectively. The value  $Q = 243.6$  kJ/mole calculated in the present work is somewhat higher than in the other studies. However, comparing the data presented, we see that the quantity  $Q$  depends much of the method of boronizing. In addition, it has been shown in [33 – 35] that the value of  $Q$  varies with the boron potential in the saturating medium, with the chemical composition of the substrate material, with the method of preparation of surface of this material, with the type and the size distribution of the boriding powders, and with other factors. This explains the difference in the results obtained in our study and presented in other works.

We used the calculated values of  $Q$  and  $K_0$  to obtain an empirical equation for predicting the thickness of the boride layer as a function of the time and the temperature of the boriding process for steel 16MnCr5, i.e.,

$$d = 19.36 \times 10^{-2} \times \sqrt{t \exp\left(-\frac{29299.9}{T}\right)}$$

1123 K <  $T$  < 1223 K. (3)

This expression can be used for assigning the process parameters for boriding of steel 16MnCr5 under industrial conditions.

## CONCLUSIONS

1. We have studied the kinetics of boriding of low-alloy steel 16MnCr5 at 1123, 1173 and 1223 K for 2, 4 and 6 h in powder mixtures with the use of an Ekabor-II agent.

2. The boride layer formed on the surface of steel 16MnCr5 has a saw-tooth morphology and a homogeneous dense structure and is represented by iron borides (FeB, Fe<sub>2</sub>B), chromium boride (Cr<sub>2</sub>B) and manganese boride (MnB). The thickness of the layer varies from 24 to 159 μm depending on the temperature and the duration of the boronizing.

3. Boriding raises the hardness of the surface of the steel by about a factor of 5; the yield strength and the ultimate tensile strength grow considerably, and the elongation decreases somewhat. The fracture energy in the impact bending tests increases by a factor of 2 – 4 depending on the treatment mode.

4. We have calculated the activation energy of boron diffusion  $Q = 243.6$  kJ/mole and the pre-exponential factor  $K_0 = 3.75 \times 10^{-2}$  m<sup>2</sup>/sec and used these values to derive an empirical equation for predicting the thickness of boride layer on steel 16MnCr6 for the specified time and temperature of the process under industrial conditions.

## REFERENCES

- N. Mohan and S. Arul, "Effect of cryogenic treatment on the mechanical properties of alloy steel 16MnCr5," *Mater. Today Proc.*, **5**, 25265 – 25275 (2018).
- S. Arunkumar, M. Chandrasekaran, V. Muthuraman, and T. Vinod Kumar, "Study properties and mechanical behavior of the shaft material 16MnCr5," *Mater. Today Proc.*, **37**, 2458 – 2461 (2021).
- I. Kováč, R. Mikuš, J. Žarnovský et al., "Creation of wear resistant boride layers on selected steel grades in electric arc remelting process," *Kovove Mater.*, **52**, 387 – 394 (2014).
- Cm. Vivek, "Influence of carburizing and carbonitriding in 16MnCr5 to enhance mechanical properties," *Int. J. Innov. Eng. Technol.*, **7**, 261 – 266 (2016).
- A. K. Litoria, C. A. Figueroa, L. T. Bim et al., "Pack-boriding of low alloy steel: microstructure evolution and migration behavior of alloying elements," *Philos. Magaz.*, **100**, 353 – 378 (2020).
- W. J. Nam and H. C. Choi, "Effect of Si on mechanical properties of low alloy steels," *Mater. Sci. Technol.*, **15**, 527 – 530 (1999).
- N. Okkubo, K. Miyakusu, Y. Uematsu, and H. Kimura, "Effect of alloying elements on the mechanical properties of the stable austenitic stainless steel," *ISIJ Int.*, **34**, 764 – 772 (1994).
- R. Kara, F. Colak, and Y. Kayali, "Investigation of wear and adhesion behaviors of borided steels," *Trans. Indian Inst. Met.*, **69**, 1169 – 1177 (2016).
- I. E. Campos-Silva, and G. A. Rodríguez-Castro, "Boriding to improve the mechanical properties and corrosion resistance of steels," in: *Thermochemical Surface Engineering of Steels, Improving Materials Performance* (2015), pp. 651 – 702.
- F. Dokumaci, I. Ozkan, and B. Onay "Effect of boronizing on the cyclic oxidation of stainless steel," *Surf. Coat. Technol.*, **232**, 22 – 25 (2015).
- I. Yegen and M. Usta, "The effect of salt bath cementation on mechanical behavior of hot-rolled and cold-drawn SAE 8620 and 16MnCr5 steels," *Vacuum*, **85**, 390 – 396 (2013).
- C. Cetinkaya and U. Arabaci, "Flash butt welding application on 16MnCr5 chain steel and investigations of mechanical properties," *Mater. Des.*, **27**, 1187 – 1195 (2006).
- A. Calik, N. Ucar, A. Kosaaslan, and S. Karakas, "Effect of interrupted boriding on microstructure and mechanical properties of 16MnCr5 steel," *Surf. Rev. Lett.*, **25**, 1 – 6 (2018).
- I. Gunes and I. Yildiz, "Rate of growth of boride layers on stainless steel," *Oxid. Commun.*, **38**, 2189 – 2198 (2015).
- M. N. Treskina and L. F. Dolgikh, "Microhardness and defectiveness of solid-solution crystals of alkali halide compounds of the system KCl – KBr," *Soviet Phys. J.*, **9**, 17 – 19 (1966).
- A. Gaber, N. Afify, S. M. El-Halawany, and A. Mossad, "Studies on Al – Mg solid solutions using electrical resistivity and microhardness measurements," *Eurp. Phys. J. Appl. Phys.*, **7**, 103 – 109 (1999).
- A. Calik, A. Duzgun, A. E. Ekinici, et al., "Comparison of hardness and wear behaviour of boronized and carburized AISI 8620 steels," *Acta Phys. Polonica A*, **116**, 1029 – 1032 (2009).
- R. Nora, T. M. Zine, K. Abdelkader, et al., "Boriding and boronitrocarburising effects on hardness, wear and corrosion behavior of AISI 4130 steel," *Revista Matéria*, **24**, P. 1 – 11 (2019).
- X. Q. Zheng, Y. Liu, J. Li, et al., "Boride precipitation and mechanical behaviour of high boron stainless steel with boron and titanium additions," *Int. J. Mater. Product Technol.*, **51**, 332 – 344 (2015).
- A. Calik, N. Ucar, K. Delikanli, et al., "Boride kinetics and mechanical properties of borided commercial purity nickel," *Indian J. Eng. Mater. Sci.*, **24**, 362 – 368 (2015).
- N. M. Sultan, I. Jauhari, and M. F. M. Sabri, "Mechanical properties of superplastic thin boronised duplex stainless steel (DSS)," *Mater. Res. Express*, **6**, 1 – 9 (2019).

22. A. Calik, F. Taylan, O. Sahin, and N. Ucar, "Comparison of mechanical properties of boronized and vanadium carbide coated AISI 1040 steels," *Indian J. Eng. Mater. Sci.*, **16**, 326 – 330 (2019).
23. J. Hou, J. Fan, H. Yang, et al., "Deformation behavior and plastic instability of boronized  $Al_{0.25}CoCrFeNi$  high-entropy alloys," *Int. J. Minerals, Metall. Mater.*, **27**, 1363 – 1370 (2020).
24. I. Gunes, M. Keddami, R. Chegroune, and M. Ozcatal, "Growth kinetics of boride layers formed on 99.0% purity nickel," *Bull. Mater. Sci.*, **38**, 1113 – 1118 (2020).
25. M. Keddami and M. Kulka, "Simulation of boriding kinetics of AISI D2 steel using two different approaches," *Metal Sci. Heat Treat.*, **61**, 756 – 763 (2020).
26. N. Ucar, O. B. Aytar, and A. Calik, "Temperature behavior of the boride layer of a low carbon microalloyed steel," *Mater. Technol.*, **46**, 621 – 625 (2012).
27. M. Ortiz-Domínguez, O. A. Gómez-Vargas, G. Ares de Parga, et al., "Modeling of the growth kinetics of boride layers in powder-pack borided ASTM A36 steel based on two different approaches," *Adv. Mater. Sci. Eng.*, **6**, 1 – 12 (2019).
28. M. Keddami, M. Ortiz-Domínguez, O. A. Gómez-Vargas, et al., "Kinetic study and characterization of borided AISI 4140 steel," *Mater. Technol.*, **49**, 665 – 672 (2015).
29. S. Sen S, U. Sen, and C. Bindal, "The growth kinetics of borides formed on boronized AISI 4140 steel," *Vacuum*, **77**, 195 – 202 (2015).
30. Z. Nait Abdellah, Z. Keddami, and A. Elias, "Evaluation of the effective diffusion coefficient of boron in the  $Fe_2B$  phase in the presence of chemical stress," *Int. J. Mater. Res.*, **104**, 260 – 265 (2013).
31. M. Ortiz-Domínguez, M. Keddami, M. Elias-Espinosa, et al., "Pack-boriding of AISI P20 steel: estimation of boron diffusion coefficients in the  $Fe_2B$  layers and tribological behavior," *Int. J. Surf. Sci. Eng.*, **11**, 563 – 585 (2017).
32. Y. Kayali, "Investigation of diffusion kinetics of borided AISI P20 steel in micro-wave furnace," *Vacuum*, **121**, 129 – 134 (2016).
33. S. Karakas, A. Gunen, E. Kanca and E. Yilmaz, "Boride layer growth kinetics of AISI H13 steel borided with nano-sized powders," *Arch. Metall. Mater.*, **63**, 159 – 165 (2018).
34. V. Jain and G. Sundararajan, "Influence of the pack thickness of the boronizing mixture on the boriding of steel," *Surf. Coat. Technol.*, **149**, 21 – 26 (2002).
35. C. M. Brakman, A. W. J. Gommers, and E. J. Mittemeijer, "Boriding of Fe and Fe–C, Fe–Cr, and Fe–Ni alloys; Boride-layer growth kinetics," *J. Mater. Res.*, **4**, 1354 – 1370 (1989).